Contact Information

Andrea Da Ronch PhD MSc BSc MAIAA FHEA

New Frontiers Fellow, Lecturer of Aircraft Structural Design and Aeroelasticity

Faculty of Engineering and the Environment, University of Southampton, Southampton, SO17 1BJ, UK

Email: a.da-ronch@soton.ac.uk

Phone number: +44 (0)23 8059 4787

Marco Panzeri

Research Engineer

Noesis Solutions N.V., 3001 Leuven, Belgium

Email: marco.panzeri@noesissolutions.com

M. Anas Abd Bari

PhD Student

Faculty of Engineering and the Environment, University of Southampton, Southampton, SO17 1BJ, UK

Email: Anas.Abd-Bari@soton.ac.uk

Roberto d'Ippolito

Research and Innovation Manager

Noesis Solutions N.V., 3001 Leuven, Belgium

Email: roberto.dippolito@noesissolutions.com

Matteo Franciolini

PhD Student

Dipartimento di Ingegneria Industriale e Scienze Matematiche, Universitá Politecnica delle Marche, I-60131, Ancona, Italy

Email: m.franciolini@pm.univpm.it

Adaptive Design of Experiments for Efficient and Accurate Estimation of Aerodynamic Loads

Abstract

Purpose – The purpose of this paper is to document an efficient and accurate approach to generate aerodynamic tables using computational fluid dynamics. This is demonstrated in the context of a concept transport aircraft model.

Design/methodology/approach – Two design of experiments algorithms in combination with surrogate modelling are investigated. An adaptive algorithm is compared to an industry-standard algorithm used as benchmark. Numerical experiments are obtained solving the Reynolds-averaged Navier-Stokes equations on a large computational grid.

Findings – This study demonstrates that a surrogate model built upon an adaptive design of experiments strategy achieves a higher prediction capability than that built upon a traditional strategy. This is quantified in terms of the sum of the squared error between the surrogate model predictions and the computational fluid dynamics results. The error metric is reduced by about one order of magnitude compared to the traditional approach.

Practical implications – This work lays the ground to obtain more realistic aerodynamic predictions earlier in the aircraft design process at manageable costs, improving the design solution and reducing risks. This may be equally applied in the analysis of other complex and non-linear engineering phenomena.

Originality/value – This work explores the potential benefits of an adaptive design of experiment algorithm within a prototype working environment, whereby the maximum number of experiments is limited and a large parameter space is investigated.

Keywords Design of Experiments; Adaptive Sampling; Surrogate Model; Computational Fluid Dynamics; Transonic Cruiser; Turbulence Model.

Paper type *Research paper*.

Introduction

Accurate predictions of aerodynamic loads are generally needed as early as possible during the aircraft design process. For a number of flight conditions prescribed by certification authorities, aerodynamic loads form a set of critical loads that are used to size aircraft structural components (Pettit, 2004). It is critical to limit the uncertainty associated with critical aerodynamic loads because: i) if the critical loads are underestimated, as revealed following flight test, then expensive re-design is often required incurring the costs and penalties arising from programme delay; and ii) if the critical loads are overestimated, the aircraft will be heavier than needed with degraded performances.

Traditionally, the aircraft design process relies heavily on semi-empirical relations and linear assumptions. The reason for this is that, at the early stage of the design process, designers explore a large parameter space resulting in a large number of numerical evaluations (Knill, 1999). Speed requirements dominate over accuracy. As the design parameters are tightened and addressed in increasing detail, the need for improved realism of predictions calls for higher fidelity aerodynamic models. Despite the availability of high performance computing (HPC) facilities, the routine use of computational fluid dynamics (CFD) is yet restricted to a pre-defined (small) number of configurations. Two remarkable studies are those of (Rogers, 2003) at NASA Ames and of (Rhew, 2007) at NASA Langley. The reasons that linear methods have cornered the industrial aircraft design process are two-fold. First, linear methods are corrected to account for un-modelled flow physics. Corrections have been calibrated using a number of previous aircraft configurations, and high confidence exists. The second reason is that linear methods are fast enough for parametric searches, and their analysis setup is straightforward practically building on a simplified description of the lifting surfaces.

The work presented in this paper addresses the problem to efficiently use CFD as source of the aerodynamic predictions. For a representative parameter space, the problem consists of maximising the information extracted from a limited number of CFD analysis. Several techniques are nowadays available in order to design the virtual experimental campaigns in an efficient and effective way. These include: i) orthogonal design techniques, e.g. fractional, full-factorial and face-centred central-composite design (Knill, 1999), in which the design points are chosen deterministically before running the virtual experiments; and ii) random methods, e.g. Monte Carlo sampling (Giunta, 2003) and Latin Hypercube (LH) (McKay, 1979), where the location of the design points is chosen randomly. The main limitation associated with traditional orthogonal and random design of experiments (DOE) techniques lies in the fact that the samples to be evaluated are chosen all at the same time, based only on information that is available before running the numerical explorative campaign. Since the knowledge available before running the DOE is often very limited, this approach makes impossible to know in advance the optimal number of samples and the location of the design points that are required in order to achieve a given accuracy in the response surface model built upon the results of the virtual experiments. A possible problem arising in this context is the so-called under-sampling effect, where the number of design points and their locations do not provide sufficient information to build a response surface function with the desired level of accuracy (Giunta, 2003). This behaviour is typically observed when design points are not distributed with sufficient density in those regions of the parameter space where the output model is characterised by a pronounced non-linearity. The opposite effect, named over-sampling, is encountered when the level of accuracy associated with the response surface model could have been achieved by running a smaller number of experiments (Crombecq, 2009). This happens, for example, when the distribution of the design points is too dense and leads to unnecessary and avoidable computational burdens.

A feasible way to mitigate the appearance of these problems consists of adopting a more advanced algorithm, such as the adaptive DOE (ADOE) (Akram, 2016). This a self-learning algorithm which makes use of an iterative procedure and is capable to: i) identify from previous runs the regions of the design space where the output model is characterised by stronger non-linearities; and ii) select a new batch of design points by maximising the (expected) information content associated with this new set of simulations. Previous applications of ADOE techniques to CFD problems can be found in (Da Ronch, 2011), (Ghoreyshi, 2013) and (Mackman, 2013). In this work, we propose to employ an ADOE methodology to identify the locations of CFD analyses that provide the best approximation of the objective function. The test case is for a complete aircraft configuration which is run on the HPC of the University of Southampton[1].

Test Case

The test case is for the transonic cruiser (TCR) model that was conceived during the Simulating Aircraft Stability and Control Characteristics for Use in Conceptual Design (SimSAC) project (Rizzi, 2011). The TCR is a conceptual design of a civil transport aircraft operating at a target Mach number of 0.97, featuring low relaxed static stability boundaries, and low manoeuvre and trim drag. The initial concept proposed by SAAB was for a conventional tailed configuration, which revealed the need for a large horizontal tail deflection affecting significantly trim drag. The evolution from the initial geometry to the final configuration, which includes an all-moving canard for longitudinal control, may be found in (Rizzi, 2011b).

A wind tunnel model of the TCR aircraft was built in a 1:40 scale compared to the full scale aircraft. A schematic of the TCR design and the sign convention adopted in this work are shown in Figure 1. The apex positions of the canard and main wing are, respectively, at 12 and 26% of the fuselage length. The close proximity of the canard with the main wing originates strong interference effects of the flow past the canard impinging on the main wing.

[1] IRIDIS at the University of Southampton is in the World's Top500 ranking and is the largest HPC facility in the U.K. after the national supercomputer. In total, it consists of 12320 processor-cores providing 250 TFlops peak.

Figure 1 TCR wind tunnel model (Khrabrov, 2010); (Reproduced with permission)

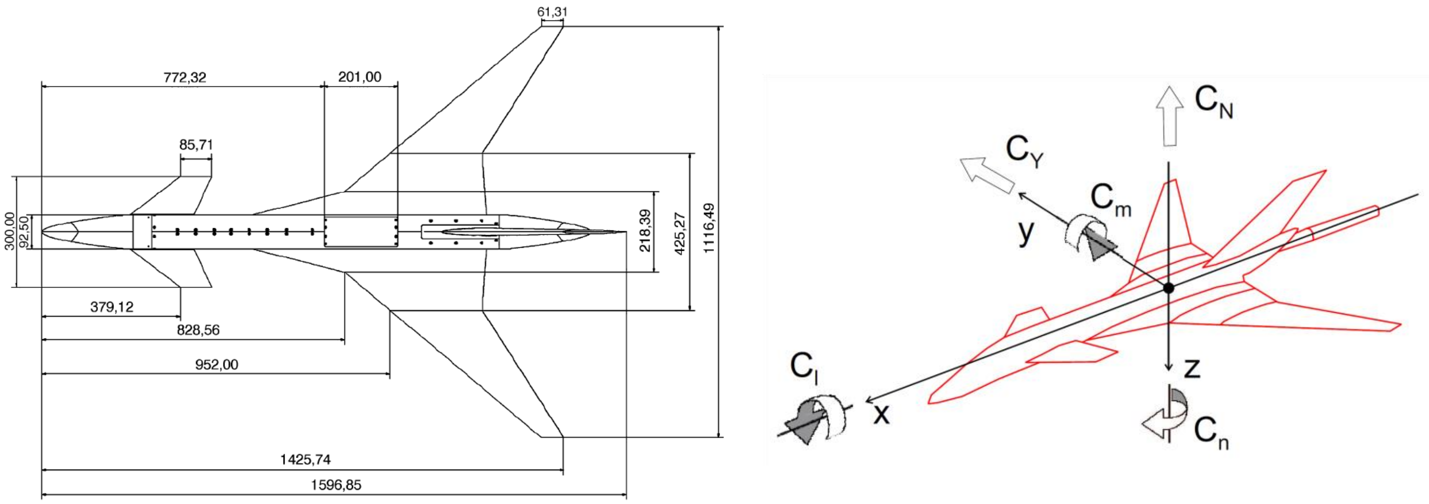

(a) TCR model top view (dimensions in millimetres) (b) Body frame of reference

Numerical analyses presented in this work were obtained for the TCR wind tunnel model geometry. Reference values are summarised in Table 1. The geometry features a symmetric aerofoil for the canard, and a cambered one for the main wing. The moment reference point is measured from the aircraft nose, positive downstream.

Table 1 Reference values of the TCR wind tunnel model

Parameter	Value
Model scale	1:40
Reference area [m^2]	0.3056
Wing span [m]	1.12
Mean aerodynamic chord [m]	0.2943
Moment reference point [m]	0.87475
Fuselage length [m]	1.597

Experimental Investigations

Experimental investigations of the steady and unsteady aerodynamic characteristics at low speed were performed in the T-103 wind tunnel facility at the Central Aerohydrodynamic Institute (TsAGI), see Figure 2. The wind tunnel has an open jet working section of the continuous type with an elliptical cross section, 4.0 m x 2.33 m.

Figure 2 TCR wind tunnel model tested in TsAGI (Khrabrov, 2010); (a) large amplitude pitch oscillations dynamic rig, and (b) 90 deg bank angle for static aerodynamic characteristics; (Reproduced with permission)

(a) Canard-off configuration (b) Canard-on configuration

Several configurations of the wind tunnel model were tested to evaluate the influence of single components (vertical tail and canard wing) on the overall performance. The experimental measurements included the investigation of the static aerodynamic characteristics, unsteady aerodynamic derivatives, and unsteady non-linear aerodynamic characteristics during large amplitude oscillations. In particular, static measurements were carried out at a wind tunnel flow velocity of 40 m/s in a wide range of angles of attack (-10.0 deg $\leq \alpha \leq 40.0$ deg, with $\Delta\alpha = 2.0$ deg) and sideslip angles (-16.0 deg $\leq \beta \leq 16.0$ deg, with $\Delta\beta = 2.0$ deg). The full dataset of wind tunnel measurements is described in (Khrabrov, 2011), which also discusses the data processing technique. No information on measurement accuracy and uncertainty are, however, given.

It is worth noting that no transition tripping was installed in the wind tunnel model, and that the leading edge of all lifting surfaces is round. As discussed below, the combination of these two aspects makes the prediction of the TCR aerodynamic characteristics challenging from a numerical standpoint. It is well-known that the vortical flow behaviour around delta wings with a round leading edge is significantly different from that around wings with a sharp leading edge (Vallespin, 2011). The separation line is fixed for a sharp leading edge, but depends highly on Reynolds number, surface roughness, leading edge bluntness and sweep angle for a round leading edge. Wind tunnel tests were run at a freestream speed of 40 m/s, which corresponds at sea level to a Mach number of 0.117 and a Reynolds number of 0.778 million based on the mean aerodynamic chord of the wind tunnel model.

Numerical Investigations

Numerical investigations reported in (Da Ronch, 2011), (Da Ronch, 2012) and (Mialon, 2011) focussed at comparing steady and unsteady predictions of the aerodynamic loads with available experimental measurements. (Da Ronch, 2012) employed a modified version of the k-ω turbulence model and a multi-block structured grid with 8.5 million grid points.

Predictions for steady results were first validated. The attention was then addressed for unsteady aerodynamics. Numerical results of aerodynamic derivatives for small oscillation amplitudes were presented, followed by results for large amplitude motions. Dependencies of dynamic characteristics on mean angle of attack and reduced frequency were investigated. Computations were for the wind tunnel model with vertical tail and un-deflected canard wing. To the authors' knowledge, this is the only original work that performed unsteady time domain calculations based on Reynolds-averaged Navier-Stokes (RANS) modelling to extract dynamic derivatives. In (Mialon, 2011), experimental and numerical research activities for the determination of dynamic derivatives were reviewed for two aircraft configurations, including the TCR model. In addition to the unsteady RANS (URANS) results of (Da Ronch, 2012), the reference included results from linear aerodynamic models based on a panel method. (Da Ronch, 2011) discussed current state-of-the-art methods to generate aerodynamic tables for flight simulation. For the TCR model, the ability to combine aerodynamic databases of different fidelity levels into a single database was demonstrated. In total, 270 CFD simulations were run, and combined with linear aerodynamics that provided quantitative trends of the aerodynamic loads across the flight envelope at very low computational cost.

Computational Fluid Dynamics Solver

The flow solver used in this work is `Ansys Fluent` (version 14.5). The reason to use a commercial solver, opposed to previous work done by the first author with research codes, is to demonstrate the seamless integration of the ADOE methodology with a well-established, widely-available software tool. We hope this demonstration will facilitate the adoption of the ADOE methodology in the analysis of other complex and non-linear engineering phenomena.

The low Reynolds number of the operating wind tunnel conditions ($M = 0.117$ and $Re = 0.778 \cdot 10^6$) and the blunt leading edge geometry of the TCR wind tunnel model make the prediction of the resulting turbulent flow difficult, especially for what concerns the flow separation near the wing leading edge. No transition tripping was used in the wind tunnel model. Without other information, all simulations herein reported were run assuming fully turbulent flow. The one-equation Spalart-Allmaras turbulence model was used in this study. The model provides the turbulent viscosity to be added to the viscous terms of the Navier-Stokes equations and mimics the effects of the inertial turbulent transport on the mean flow. The details of the turbulence model can be found in (Spalart, 1992). All computations were run in double precision.

An unstructured grid for the half-model configuration was generated with 10 million points. Jobs were run on IRIDIS on 32 processes and about 10 hours of wall clock time. The flow field has a semi-spherical shape with the far-field located on average at 170 times the mean aerodynamic chord from the aircraft geometry. This ensures avoiding the flow field disturbances propagate beyond the far-field boundary. Boundary conditions were set to symmetry plane on the vertical plane of symmetry, and to no-slip adiabatic wall on the aircraft surface. At the inlet, the pressure gradient was set to zero while the flow velocity set to the free-stream conditions. The grid, show in Figure 3, was chosen after a grid convergence study was carried out, demonstrating independence of the results obtained with the current grid size.

Figure 3 Surface grid of the TCR wind tunnel model

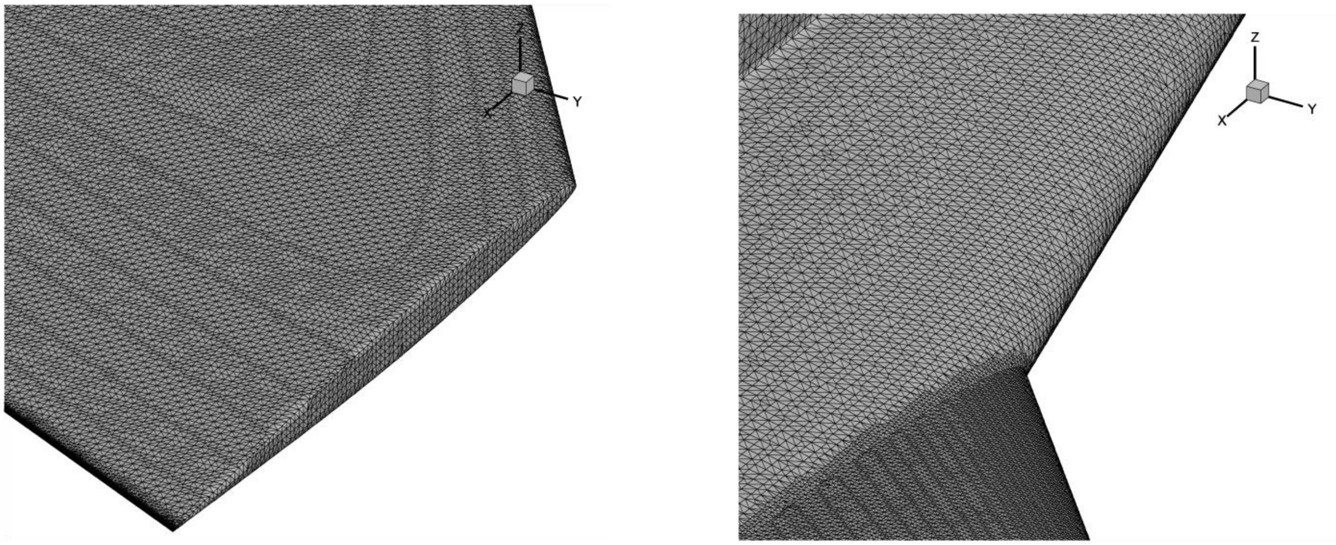

(a) Canard wing tip (b) Kink on main wing

In all cases, computed results are for zero side-slip angle (β = 0.0 deg) and the influence of the rear sting was ignored. The moment reference point was set at 54.78% of the fuselage length from the foremost point.

Design of Experiments

For the size of the computational grid used in this work, a well-converged simulation is computed at high computing times. The generation of the aerodynamic database across the flight envelope adopts an ADOE technique, which is detailed in the following. A review of the LH method is also given, as it is used as benchmark in order to assess the improvements achieved by the ADOE technique compared with a more traditional, industry-standard DOE approach.

Adaptive Design of Experiments

The ADOE is an iterative DOE technique in which the data produced during previous iterations are analysed in order to distribute the design points of the next iteration in areas of the parameters space considered of interest. The ADOE is a self-learning algorithm that is driven by two opposite factors: space-learning and feature-learning. Space-learning is the act of exploring the domain to find areas of the design space that have not yet been explored. The main goal of space learning is to fill the design space uniformly, avoiding the need of any information about the response of the model. `maximin` sampling (Johnson, 1990) is the technique implemented to support the space-learning aspect of our ADOE algorithm. Conversely, the goal of feature-learning is to add new samples in areas of the domain that have already been identified as interesting for some reason. Feature-learning is then used to improve the accuracy of the surrogates in given areas that can be difficult to model efficiently (discontinuities, steep slopes, etc.). In our implementation of the ADOE, the feature-learning aspect provides indication of where the new set of points should be distributed and is supported by two different techniques developed in-house: Model Error Sampling (MES) and Non-Linearity Search (NLS).

With MES, multiple surrogate models are built over the domain. We consider Kriging interpolating models together with linear, cubic and thin-plate Radial Basis Functions (RBF). The areas of major interest are identified as those where the variance between these surrogate models is higher. The NLS algorithm entails the computation of a hessian approximation at a given number of control points within the design space by means of the best interpolating model identified up to the given iteration, which is calculated analytically or numerically, depending on the mathematical formulation of the response model. The areas of major interest are then identified by evaluating the misfit between the simulated output and the output estimated by means of the local linear approximation at nearby samples.

A balanced strategy, combining space- and feature-learning, is adopted in the current ADOE methodology whereby the locations of 50% of the points to be selected for a new iteration is chosen according to the space-learning strategy while the remaining 50% of the design points is distributed on the basis of the feature-learning algorithms. The ADOE strategy, illustrated in Figure 4, consists of the following steps:

1. *Initialisation*. An initial set of samples is drawn according to a traditional (non-adaptive) DOE technique. In this work, this is performed by adopting a LH scheme.
2. *Build surrogate models*. A set of surrogate models is built according to the available simulation results and the regions of major interest are identified according to the MES and NLS algorithms.
3. *Adaptive sampling*. A new set of design points is chosen according to the information obtained at Step 2, and the trade-off strategy between space- and feature-learning that was chosen before running the algorithm.
4. *Check termination criteria*. If the termination criteria are not satisfied, a new batch of experiments is run and the algorithm restarts from Step 2. Suitable termination criteria may consist of: i) maximum number of model evaluation; or ii) accuracy of the surrogate models, measured in terms of misfit between the simulated outputs and the output calculated from the surrogate models. In the current implementation, this metric is calculated on the basis of an extra set of samples that are used exclusively for this purpose, called “validation set”.

Figure 4 Schematic of the ADOE framework employed in this work

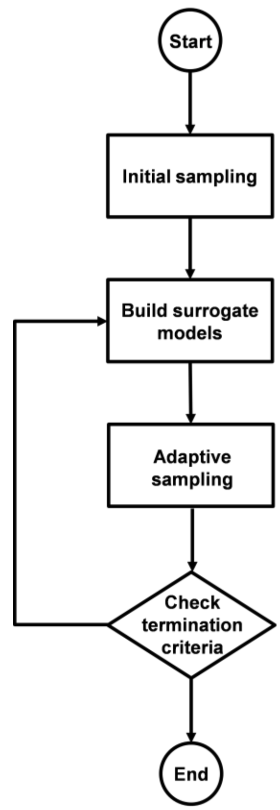

Similarly to many existing random sampling design schemes, the behaviour of the ADOE algorithm is non-deterministic and is influenced by the presence of random components. To assess the robustness of the ADOE algorithm and the impact of this inherent randomness on the quality of the results, a suite of analytical test functions (e.g. Ackley, Rosenbrock, Goldstein-Price, among others) are considered (Surjanovic and Bingham, 2013). For each of these test functions, several runs of the ADOE algorithm were performed by adopting three different values of the random seed and considering different number of design points (up to 1,000 points). The quality of the response surface functions built on the basis of the outputs calculated at these design points was then assessed by measuring the misfit between the response surface model output and the true output at 10,000 validation points, regularly distributed inside the design space. To assess the quality of ADOE against a more traditional DOE scheme, the same analysis was performed also by considering a LH algorithm. Figure 5 shows the sum of the squared errors (SSE) at the validation points versus the number of design points for three runs of ADOE and LH performed with different seed numbers. The results shown in Figure 5 were obtained for the Ackley test function. It was found that: i) the impact of the random components of the ADOE algorithm on the quality of the sampling scheme is negligible; and ii) the relative improvement of ADOE with respect to LH, measured in terms of the SSE metric, is robust. Similar findings were obtained for other types of test functions, not reported here for conciseness.

Figure 5 Sum of squared errors (SSE) at 10,000 validation points versus the number of design points for three runs of ADOE and LH performed with different seed numbers; the test function is based on the Ackley function

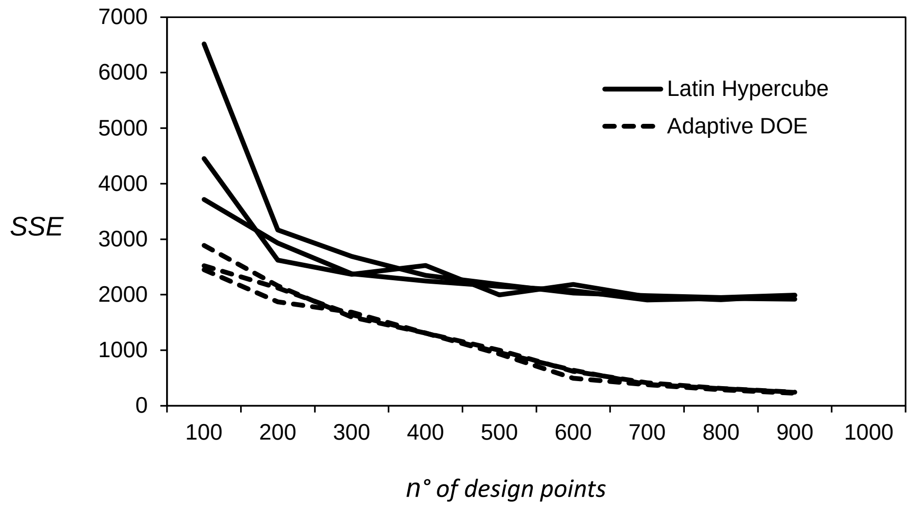

Latin Hypercube Design

The LH design (LHD) is one of the most commonly used random DOE (McKay, 1979). A LHD is constructed by dividing the range of each design parameter in *n* equally probable intervals, *n* being the number of design points. The design points are then randomly chosen in such a way that for each interval there is only one design point (Knill, 1999). This selection of design points ensures that: i) each interval is present in the design; and ii) the number of levels is maximised. One of the main advantages of LHDs is that it avoids the “collapse problem”, because if one or more of the input factors appear to be irrelevant, every point in the design still gives information about the influence of the other factors on the response. In this way, each time-consuming computer experiment adds useful information.

The intervals onto which each input dimension is subdivided may be assigned randomly or according to a custom rule. An efficient and effective way to construct a LHD is to assign the intervals in such a way that the resulting design is space-filling, i.e. the design points are spread out and do not cluster in one portion of the experimental region. In our implementation of LHD, we: i) measure the degree of spread of the design points by computing the minimal distance between two of its design points; and ii) choose the LHD which provides the maximum value of this metric. This strategy is generally referred to as `maximin` LHD (Johnson, 1990).

Results

This section is organised as follows. First, aerodynamic predictions are validated against available experimental data at wind tunnel conditions. Then, the proposed ADOE methodology is demonstrated for a prototype flight envelope.

Validation at Wind Tunnel Flow Conditions

The validation is carried out at the operating wind tunnel conditions, M = 0.117 and Re = $0.778 \cdot 10^6$. The free-stream angle of attack is varied between -10.0 and 40.0 deg, and the sideslip angle is fixed at β = 0.0 deg. Experimental data are available at a step in angle of attack of 2.0 deg, whereas simulations were performed for a smaller increment of 1.0 deg.

A preliminary study was conducted to ensure the results presented are fully converged. Two flow conditions were chosen, at 0.0 and 10.0 deg angle of attack. The independence on the number of inner iterations was assessed comparing the average value of aerodynamic coefficients in the last 1,000 iterations at three relevant check points: after 5,000, 7,500, and 10,000 iterations. The convergence of the residuals with the number of iterations is shown in Figure 6. The vertical lines in the figures indicate the intermediate check points at 5,000 and 7,500 iterations. The normal force and pitch moment coefficients, C_N and C_m, respectively, computed at 5,000, 7,500, and 10,000 iterations are reported in Table 2. It was found that the percent error, computed using the values at 10,000 iterations as reference, is well below one percent in all cases. Based on this finding, all simulation results reported herewith were obtained for 5,000 iterations.

Figure 6 Convergence of the solution residuals at two angles of attack at wind tunnel conditions (M = 0.117, β = 0.0 deg and Re = $0.778 \cdot 10^6$)

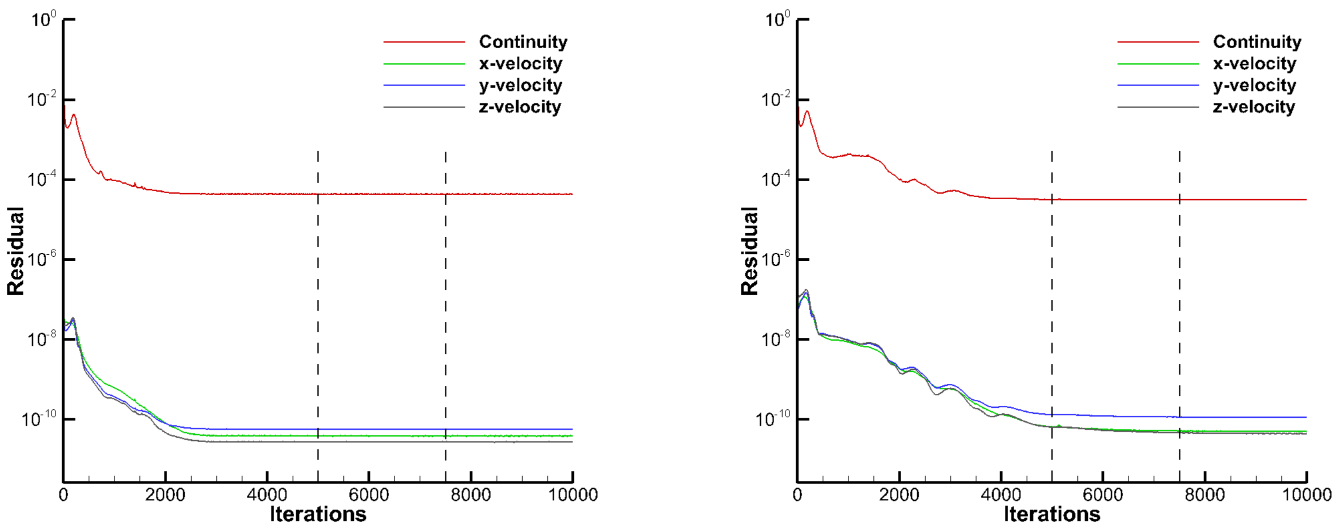

(a) α = 0.0 deg

(b) α = 10.0 deg

Table 2 Convergence of the aerodynamic coefficients with the number of iterations at wind tunnel conditions (M = 0.117, β = 0.0 deg and Re = $0.778 \cdot 10^6$)

	α = 0.0 deg		α = 10.0 deg	
Iterations	C_N	C_m	C_N	C_m
5000	$1.120 \cdot 10^{-1}$	$-9.110 \cdot 10^{-2}$	$6.435 \cdot 10^{-1}$	$-2.077 \cdot 10^{-1}$
7500	$1.120 \cdot 10^{-1}$	$-9.110 \cdot 10^{-2}$	$6.428 \cdot 10^{-1}$	$-2.070 \cdot 10^{-1}$

10000	$1.120 \cdot 10^{-1}$	$-9.110 \cdot 10^{-2}$	$6.427 \cdot 10^{-1}$	$-2.069 \cdot 10^{-1}$

The static aerodynamic characteristics are shown in Figure 7. Available wind tunnel measurements, labelled as “Exp Data” in figure, suggest that the normal force coefficient has a linear (or quasi-linear) behaviour with the angle of attack up to about 20 deg. Above this angle, the curve slope of the force coefficient decreases, until the maximum value of normal force coefficient is found at about 38 deg. The pitch moment coefficient has a strong non-linear dependence on the angle of attack. Two break points are identified, at about 6 and 20 deg. For small angles of attack, the pitch moment coefficient has a negative slope, i.e. nose-down tendency for increasing angle of attack. A first break point is found at about 6 deg, where the slope-sign changes to positive. (Mialon, 2011) attributed this to a continuously increasing lift on the canard wing, which is located upstream of the moment reference point and causes a nose-up tendency. The lightly unstable characteristics, confined between 6 and 20 deg, are then followed by a second break point, which suggests a massive flow separation.

Figure 7 Static aerodynamic characteristics of the TCR wind tunnel model at wind tunnel conditions (M = 0.117, β = 0.0 deg and Re = $0.778 \cdot 10^{6}$)

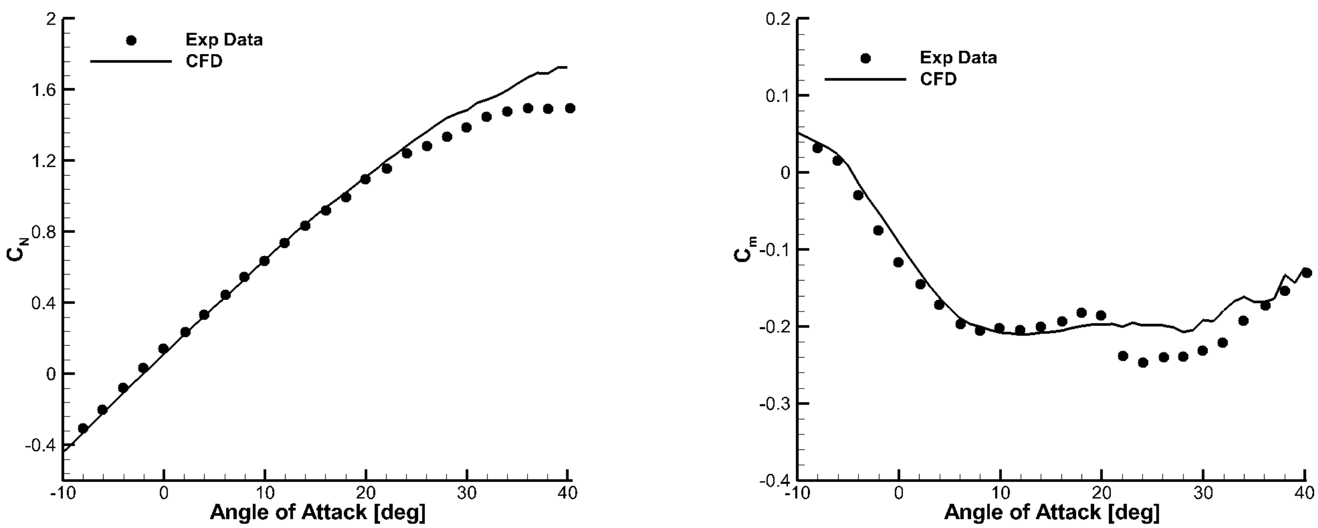

(a) Normal force coefficient

(b) Pitch moment coefficient

The comparison of the CFD results against wind tunnel measurements is excellent up to about 20 deg, as in Figure 7. Aerodynamic characteristics are well captured, including the normal force coefficient curve slope and the non-linear dependence of the pitch moment coefficient with the angle of attack. The reference point for the pitch moment coefficient is in close proximity with the location of the vortex breakdown on the main wing, which moves upstream for increasing angle of attack. Predictions of C_m are therefore very sensitive to the simulated flow features. The agreement indicates that the flow physics are simulated correctly with the turbulence model adopted up to about 20 deg. The surface signature and structure of the vortices forming over the canard and main wing are shown in Figure 8 for various angles of attack. Above α = 20.0 deg, the flow presents massively separated regions that are not modelled properly with a RANS model, requiring higher fidelity in the flow modelling as well as resolving the important unsteady effects in the flow (Righi, 2017).

Figure 8 Flow visualisation using surface pressure distribution (in Pa) and volume stream traces; for visualisation, the computational model was mirrored (M = 0.117, β = 0.0 deg and Re = $0.778 \cdot 10^{6}$)

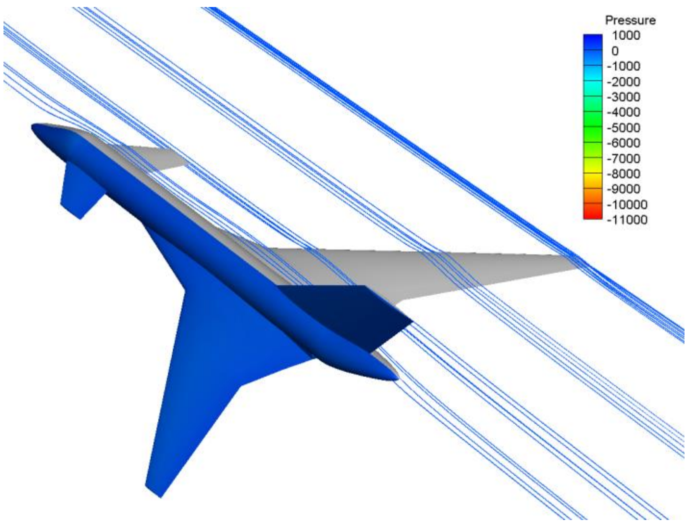

(a) α = 0.0 deg

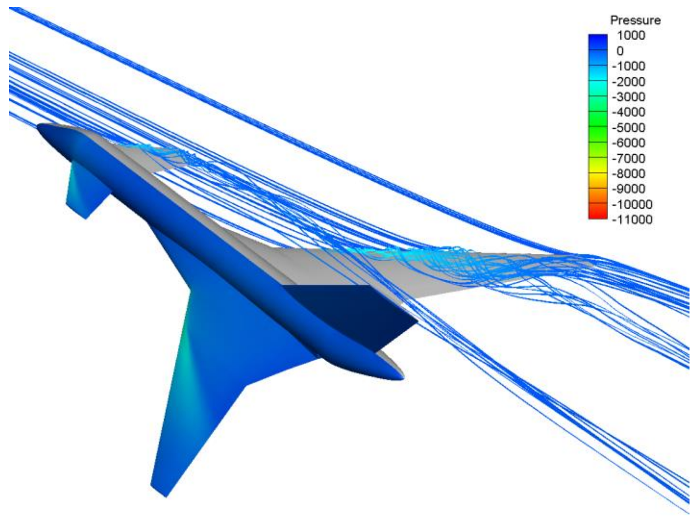

(b) α = 10.0 deg

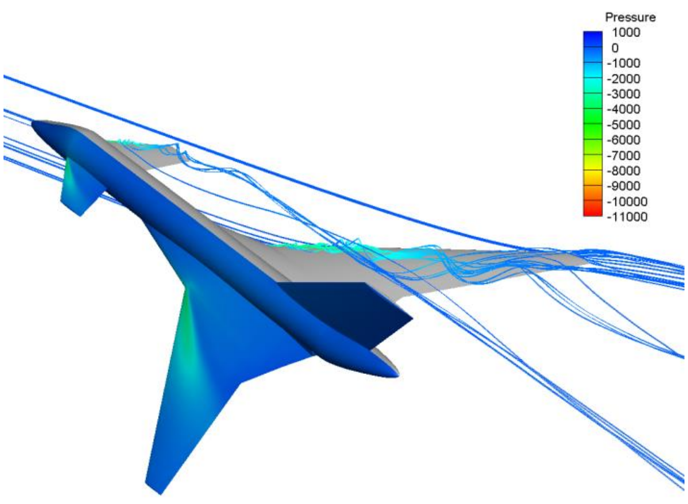

(c) α = 15.0 deg

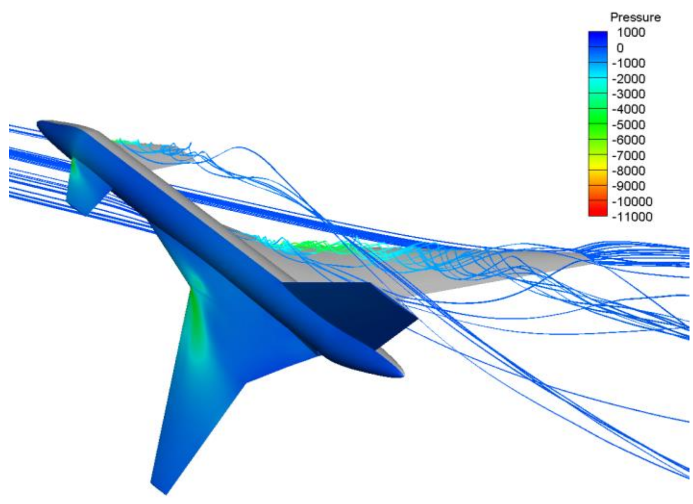

(d) α = 20.0 deg

Aerodynamic Characteristics Across the Flight Envelope

To investigate the capability of the DOE techniques, a prototypical two-dimensional parameter space was generated. Both LHD and ADOE provide the capabilities to consider the design space as a continuum. The lower and upper boundaries were defined as a function of the Mach number: α ∈ [-10.0; 40.0] deg at M = 0.117, and α ∈ [-5.0; 5.0] deg at M = 0.97.

The parameter space that is illustrated by the dashed line in Figure 9(a) is similar in size to that of (Rogers, 2003), who analysed the aerodynamics of a reusable launch vehicle (for eight Mach numbers, five sideslip angles and eight angles of attack) under the NASA's Space Launch Initiative programme.

Since the DOE techniques are designed to work on rectangular domains, it is required to: i) sample the design points on a canonical square defined within the interval [-1; 1] in both dimensions; and ii) map these points onto the physical domain by means of a bi-linear transformation. This is illustrated in Figure 9 for the parameter space of this study.

Figure 9 Bi-linear transformation mapping physical domain in (a) with canonical domain in (b); the symbols show the locations where the calculations are performed for validation purposes

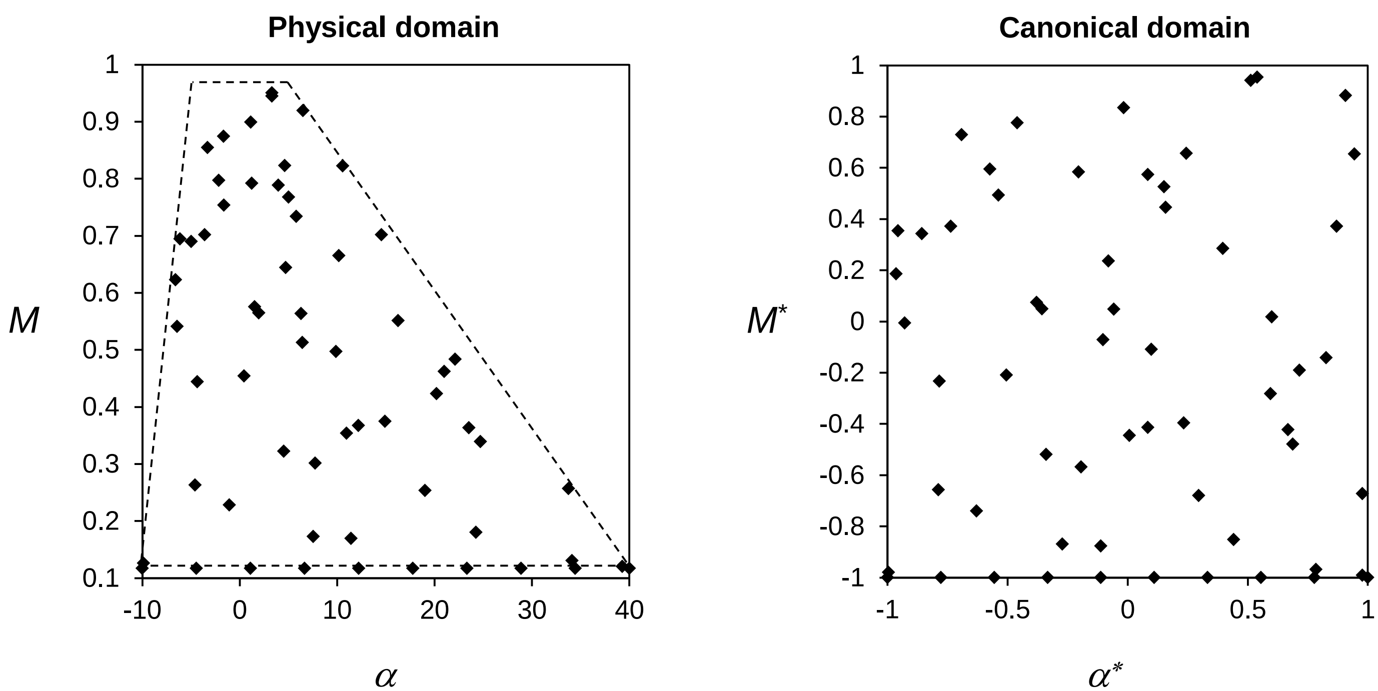

(a) Physical domain

(b) Canonical domain

The results obtained by running the two DOE techniques, each composed of 40 design points, are compared. The reasons to set a small number of design points, 40 in this case, are two-fold. First, the surrogate model built using the LHD will converge to that built using the ADOE for increasing number of design points, while the expected potential benefits of the ADOE will be for a small number of design points through an improved convergence rate (recall Figure 5). The second reason is that, practically, the maximum number of design points is limited by available hardware resources and project timescales. At NASA Langley, for example, the initial plan to analyse more than 1000 geometry configurations of a launch abort system, consisting of seven geometric parameters, was strategically reduced to 84 (Rhew, 2007).

The DOE methods are run using the algorithms implemented in the process integration and simulation framework `Noesis Optimus` (Noesis Solutions, 2015). The software is also used to automate the submission of the CFD simulations to the IRIDIS HPC. The ADOE strategy is initialized by calculating the output of a set of 10 experiments that are drawn using a LH technique. Then, the iterative procedure depicted in Figure 4 is started, and a new batch of 10 experiments is launched at each iteration until the total number of 40 experiments is reached.

The outputs obtained by running the two DOE algorithms are employed to build corresponding analytical surrogate models of C_N and C_m. In this study, the analysis is focused on one type of response surface model, which is based on cubic RBFs. Figure 10 shows the behaviour of the surrogate models obtained from LH and ADOE experiments. It was found that the response surfaces obtained for C_N are virtually the same for both approaches. This is not unexpected because the behaviour of C_N on the design variables is almost linear within the domain of interest, and therefore a good reconstruction of the system response is provided independently of the locations of the design points. On the contrary, the surrogates of C_m have substantial differences and provide distinct predictions of the target quantity, particularly, in correspondence to the lower-right corner of the investigated domain (low speed, high angles of attack). These differences can be explained by the fact that the design points employed by the ADOE algorithm: i) are more uniformly distributed within the domain of interest; and ii) provide a better coverage of the area of the domains that are typically difficult to model (corners and boundaries).

Figure 10 Surrogate response built using a cubic RBF model from the interpolation of the outputs associated with: in (a)-(b), the 40 LH experiments; and in (c)-(d), the 40 ADOE experiments

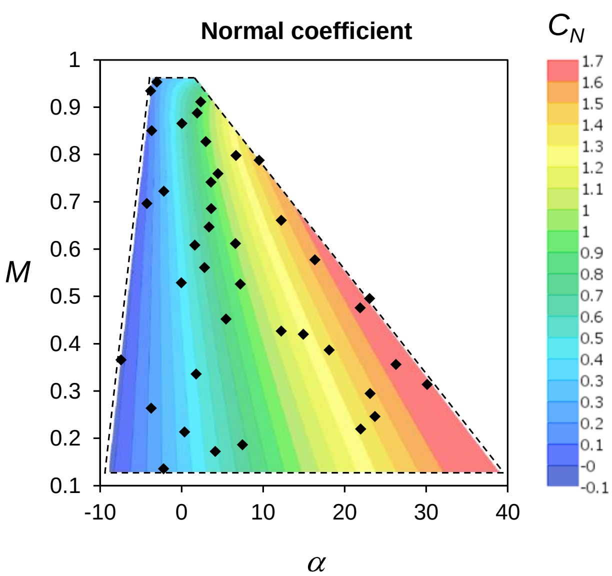

(a) Normal force coefficient / LH

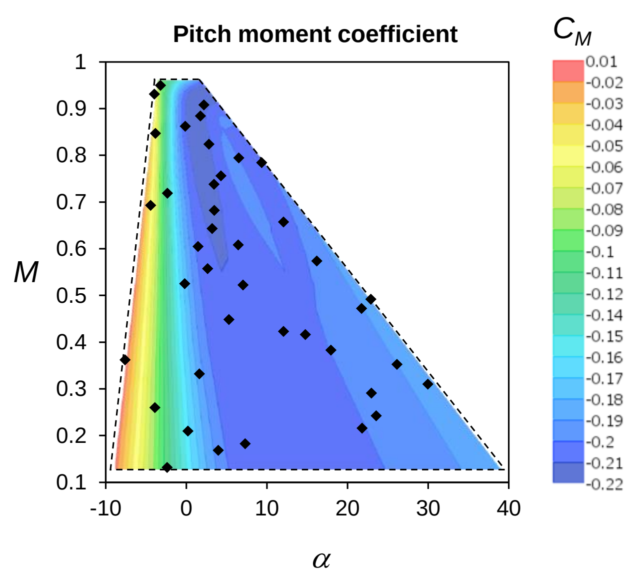

(b) Pitch moment coefficient / LH

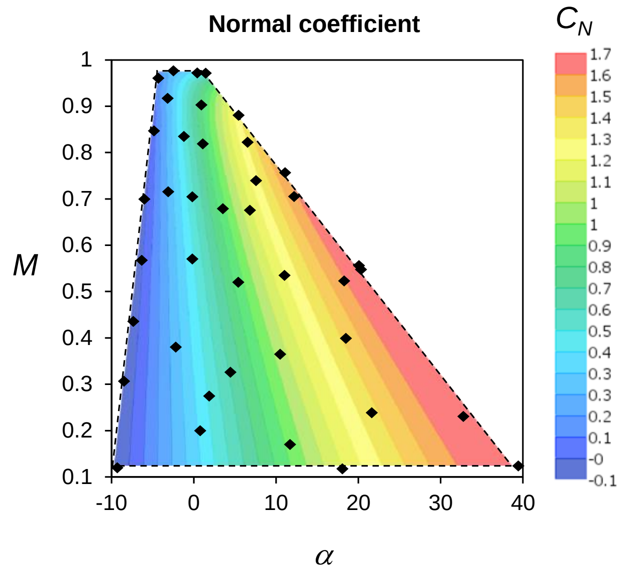

(c) Normal force coefficient / ADOE

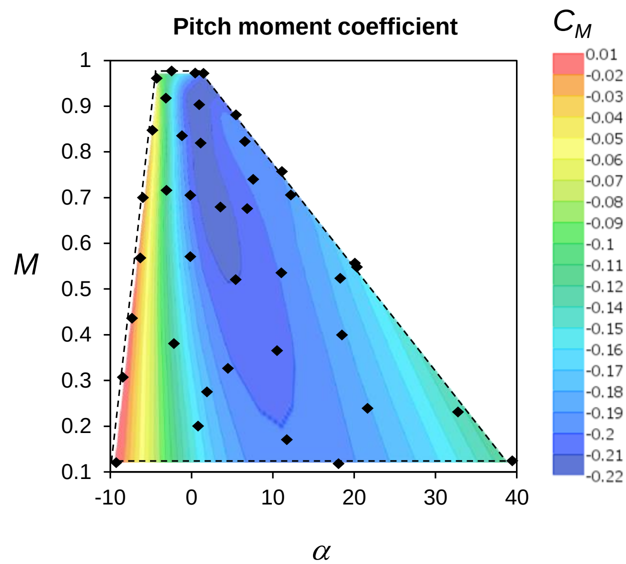

(d) Pitch moment coefficient / ADOE

The enhanced capability of the ADOE algorithm with respect to LH to distribute the design points in an intelligent way is also reflected in an improved quality of the predictions obtained from the associated surrogate models. To quantify this, an additional batch of 61 experiments, see Figure 9(a), were run for validating the quality of the surrogate models. Fifty validation points are distributed within the domain by means of a LH algorithm, with the remaining 11 points that correspond to a subset of the experiments used to validate the CFD model (M = 0.117 and $\alpha \in [-10.0; 40.0]$ deg). Figure 9 depicts the location of these validation points within the design space. The data that correspond to the wind tunnel operating conditions are particularly useful to test the ability of the surrogate models to predict the true output at the domain boundary. Besides this, we also note that considering a too large number of validation points distributed in the correspondence of the domain boundary would not provide a good and global assessment of the quality of the response surface over the entire domain. For this reason, we decided to consider only 11 points out of the 40 displayed in Figure 7. The scatter plots depicted in Figure 11 compare the outputs calculated by the surrogate models and by CFD calculation at the 61 validation points. The predictive capability of each response surface model is measured in terms of the SSE. In the figures, the dashed diagonal line indicates a perfect match between the surrogate model prediction and the CFD data. In the case of a perfect match, the SSE is zero. The scatter plots demonstrate that the surrogate models built upon the ADOE experiments are able to provide a better prediction of the system response. This difference is particularly evident by comparing the pitch moment coefficient in Figure 11(b) and (d). In Figure 11(d), data are well aligned along the dashed diagonal line, indicating a smaller error to the CFD results than achieved by the surrogate model built using the LH experiments. This is quantified in terms of SSE: the SSE value obtained from the ADOE algorithm (SSE = $3.6 \cdot 10^{-3}$) is nearly 60% smaller than the same quantity calculated using the LH algorithm (SSE = $8.7 \cdot 10^{-3}$).

Figure 11 Scatter plots obtained by comparing the outputs calculated from CFD calculations and those evaluated using the response surface models of the two output variables (C_N and C_m) for each DOE algorithm at 61 validation points

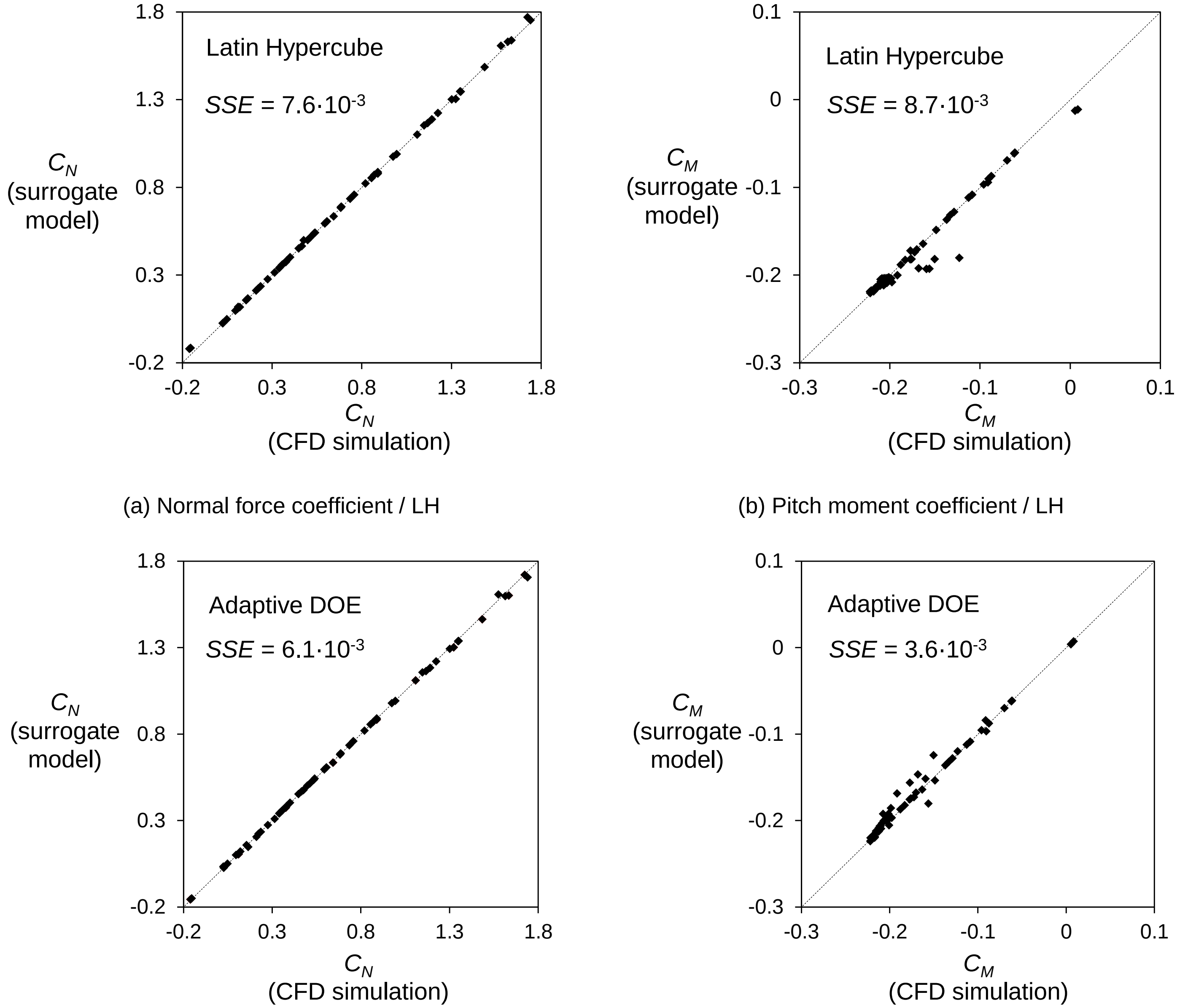

(a) Normal force coefficient / LH

(b) Pitch moment coefficient / LH

(c) Normal force coefficient / ADOE

(d) Pitch moment coefficient / ADOE

Conclusion

The work carried out in this study investigates an efficient and effective methodology to generate a full aerodynamic database for a complete aircraft model. The Reynolds-averaged Navier-Stokes equations are solved on a grid containing approximately 10 million points. Preliminary tests confirmed that results were independent of the grid spatial discretisation. Having verified that numerical results using a spatially converged grid are in good agreement with experimental data, a two-dimensional flight envelope was created. The design parameters are for the angle of attack and Mach number. The angle of attack varies with Mach number, and the range reduces for increasing Mach number. A surrogate model, based on radial basis function interpolation, was used to approximate the aerodynamic loads across the flight envelope from a total of 40 numerical results. To distribute the 40 experiments, two design of experiments strategies were investigated. The first one is a traditional Latin Hypercube approach whereby samples are randomly distributed throughout the parameter space. The second strategy is based on an adaptive design of experiments technique. To assess the accuracy of the two surrogate models, measured in terms of misfit between the numerical results using the Spalart-Allmaras turbulence model and the output of the surrogate model, an extra set of samples were used. The extra set of samples include 50 points distributed within the domain by means of a Latin Hypercube algorithm while the remaining 11 points are for the wind tunnel measurements. The data corresponding to the wind tunnel operating conditions are particularly useful to test the ability of the surrogate models to predict the true output in the correspondence of the domain boundary.

- The predictive capability of each response surface model is measured in terms of the sum of the squared error. In the case of a perfect match between the surrogate model prediction and the Reynolds-averaged Navier-Stokes data, the sum of the squared error is zero.
- It was found that the surrogate model built upon the adaptive strategy is able to provide a better prediction of the system response. This, in particular, is valid for the pitch moment coefficient that shows strong non-linear features.
- Quantitatively, for the pitch moment coefficient, the sum of the squared error value obtained from the adaptive algorithm (SSE = $3.6\cdot10^{-3}$) is nearly 60% smaller than the same quantity calculated from the Latin Hypercube algorithm (SSE = $8.7\cdot10^{-3}$). Conversely, the surrogate model built using the Latin Hypercube algorithm requires more samples (and more expensive calculations) to achieve the same error level than the surrogate model using the adaptive algorithm.

Regarding the long-term development: considering that the adaptive strategy does not incur in extra costs compared to the traditional counterpart, and that the integration within an existing environment is seamless, the authors hope this demonstration will facilitate the adoption of the adaptive design of experiments methodology in the analysis of other complex and non-linear engineering phenomena, particularly, within an industrial environment.

Acknowledgments

The authors acknowledge the use of the IRIDIS High Performance Computing Facility, and associated support services at the University of Southampton, in the completion of this work. Andrea Da Ronch is also grateful for the financial support received from the Royal Academy of Engineering under the Industrial Secondments Scheme (ISS1415\7\44). The authors also acknowledge the contribution from the following people: Adam Jirasek of the USAF for providing the grid of the TCR model; Paolo Viviani and Riccardo Lombardi of Noesis Solutions N.V. for their help with the ADOE benchmarking tests;

and Maximilien Landrain of Noesis Solutions N. V. and Elena Vataga of the University of Southampton for the deployment of Noesis Optimus on IRIDIS.

References

Akram, U., Cristofaro, M. and Da Ronch, A. (2016), “Virtual flight simulation using computational fluid dynamics”, In Marques, P. and Da Ronch, A. (Eds.), Novel Concepts in Unmanned Aircraft Aerodynamics, Flight Stability, and Control, *Wiley-Blackwell*, Chichester, GB. ESBN-10: 1118928687, ISBN-13: 978-1118928684.

Crombecq, K., Couckuyt, I., Gorissen, D. and Dhaene, T. (2009), “Space-filling sequential design strategies for adaptive surrogate modelling”, *In Proceedings of the First International Conference on Soft Computing Technology in Civil, Structural and Environmental Engineering*, Paper 50.

Da Ronch, A., Ghoreyshi, M. and Badcock, K.J. (2011), “On the generation of flight dynamics aerodynamic tables by computational fluid dynamics”, *Progress in Aerospace Sciences*, Vol. 47 No. 8, pp. 597-620. doi: 10.1016/j.paerosci.2011.09.001.

Da Ronch, A., Vallespin, D., Ghoreyshi, M. and Badcock, K.J. (2012), “Evaluation of dynamic derivatives using computational fluid dynamics”, *AIAA Journal*, Vol. 50 No. 2, pp. 470-484. doi: 10.2514/1.J051304.

Ghoreyshi, M., Cummings, R.M., Da Ronch, A. and Badcock, K.J. (2013), “Transonic aerodynamic loads modeling of X-31 aircraft pitching motions”, *AIAA Journal*, Vol. 51 No. 10, pp. 2447-2464. doi: 10.2514/1.J052309.

Giunta, A., Wojtkiewicz, S. and Michael Eldred (2003), “Overview of modern design of experiments methods for computational simulations”, *In 41st Aerospace Sciences Meeting and Exhibit, Aerospace Sciences Meetings*, AIAA Paper 2003-649, Reno, NV. doi: 10.2514/6.2003-649

Johnson, M.E., Moore, L.M. and Ylvisaker, D. (1990), “Minimax and maximin distance designs”, *Journal of Statistical Planning and Inference*, Vol. 26 No. 2, pp. 131-148. doi: 10.1016/0378-3758(90)90122-B.

Khrabrov, A., Kolinko, K., Zhuk, A. and Grishin I. (2010), “Wind tunnel test report”, SimSAC Report Deliverable D6.4-7.

Khrabrov, A.N., Kolinko, K.A., Vinogradov, Y.A., Zhuk, A.N., Grishin, I.I. and Ignatyev, D.I. (2011), “Experimental investigation and mathematical simulation of unsteady aerodynamic characteristics of a transonic cruiser model at small velocities in a wide range of angles of attack”, *Visualization of Mechanical Processes: An International Online Journal*, Vol. 1 No. 2. doi: 10.1615/VisMechProc.v1.i2.40.

Knill, D.L., Giunta, A.A., Baker, C.A., Grossman, B., Mason, W.H., Haftka, R.T. and Watsonft, L.T (1999), “Response surface models combining linear and euler aerodynamics for supersonic transport design”, *Journal of Aircraft*, Vol. 36 No. 1, pp. 75-86. doi: 10.2514/2.2415.

Mackman, T.J., Allen, C.B., Ghoreyshi, M. and Badcock, K.J. (2013), “Comparison of adaptive sampling methods for generation of surrogate aerodynamic model”, *AIAA Journal*, Vol. 51 No. 4, pp. 797-808. doi: 10.2514/1.J051607.

McKay, M.D., Beckman, R.J. and Conover, W.J. (1979), “A comparison of three methods for selecting values of input variables in the analysis of output from a computer code”, *Technometrics*, Vol. 21 No. 2, pp. 239-245. doi: 10.1080/00401706.1979.10489755.

Mialon, B., Khrabrov, A., Khelil, S.B., Huebner, A., Da Ronch, A., Badcock, K.J., Cavagna, L., Eliasson, P., Zhang, M., Ricci, S., Jouhaud, J.-C., Rogé, G., Hitzel, S. and Lahuta, M. (2011), “Validation of numerical prediction of dynamic derivatives: the DLR-F12 and the transcruiser test cases”, *Progress in Aerospace Sciences*, Vol. 47 No. 8, pp. 674-694. doi: 10.1016/j.paerosci.2011.05.002.

Pettit, C.L. (2004), “Uncertainty quantification in aeroelasticity: recent results and research challenges”, *Journal of Aircraft*, Vol. 41 No. 5, pp. 1217-1229. doi: 10.2514/1.3961.

Noesis Solutions (2015), “Optimus rev 10.17 - manual”.

Rhew, R.D. and Parker, P.A. (2007), “A parametric geometry computational fluid dynamics (CFD) study utilizing design of experiments (DOE)”, *In U.S. Air Force T&E Days*, AIAA Paper 2007-1615, Destin, FL. doi: 10.2514/6.2007-1615.

Righi, M., Da Ronch, A. and Mazzacchi, F. (2017), “Analysis of resolved turbulent scales of motion in aeroelastic problems”, *In AIAA SciTech Forum*, Grapevine, TX.

Rizzi, A. (2011), “Modeling and simulating aircraft stability and control - the SimSAC project”, *Progress in Aerospace Sciences*, Vol. 47 No. 8, pp. 573-588. doi: 10.1016/j.paerosci.2011.08.004.

Rizzi, A., Eliasson, P., Goetzendorf-Grabowski, T., Vos, J.B., Zhang, M. and Richardson, T.S. (2011b), “Design of a canard configured transcruiser using CEASIOM”, *Progress in Aerospace Sciences*, Vol. 47 No. 8, pp. 695-705. doi: 10.1016/j.paerosci.2011.08.011.

Rogers, S.E., Aftosmis, M.J., Pandya, S.A., Chaderjian, N.M., Tejnil, E.T. and Ahmad, J.U. (2003), “Automated cfd parameter studies on distributed parallel computers”, *In 16th AIAA Computational Fluid Dynamics Conference*, AIAA Paper 2003-4229, Orlando, FL. doi: 10.2514/6.2003-4229.

Surjanovic, S. and Bingham, D. (2013), Virtual Library of Simulation Experiments: Test Functions and Datasets. Retrieved December 15, 2016, from http://www.sfu.ca/~ssurjano.

Spalart, P.R. and Allmaras, S.R. (1992), “A one equation turbulence model for aerodynamic flows”, in 30th Aerospace Sciences Meeting and Exhibit, AIAA Paper 1992-439, 1992, doi: 10.2514/6.1992-439.

Vallespin, D., Da Ronch, A., Boelens, O. and Badcock, K.J. (2011), “Validation of vortical flow predictions for a UCAV wind tunnel model”, *Journal of Aircraft*, Vol. 48 No. 6, pp. 1948-1959. doi: 10.2514/1.C031385.